JOURNAL OF THE
STRUCTURAL DIVISION

PREDICTION OF HYSTERESIS OF REINFORCED CONCRETE MEMBERS

By Zdeněk P. Bažant,[1] M. ASCE and Parameshwara D. Bhat[2]

INTRODUCTION

In an earthquake, the columns and beams of a concrete building suffer large cyclic deflections. The nonlinear load-deflection characteristics govern the hysteretic damping of the earthquake motion, and their correct prediction is needed for antiseismic design. The problem is complicated by the fact that the deformations are large and cyclic, the concrete undergoes cracking and crack closing, and is subjected to triaxial stress because of the large forces that the dilatancy accompanying large shear strains induces in the stirrups.

Until recently, the constituent properties of the material have not been known sufficiently well and, for this reason, the behavior observed in the tests of concrete beams (1,6,7,8,18,21,25,28) has been the only available basis for design considerations. However, it is rather questionable to extrapolate such information to beams and load histories that differ from those tested. To obtain a prediction method, the response of reinforced concrete members must be calculated on the basis of constituent properties. Using the finite element method and the step-by-step loading technique, many investigators attacked this problem for concrete structures in general (2,9,13,14,15,16,17,23,27,29,30) and for seismic response of beams in particular (3,10,12,16,18,26). Various types of stress-strain relations for concrete and steel, and various models for steel-concrete bond, for cracking, for cracked concrete, and for the hysteresis loops in steel (with the Bauschinger effect) have been examined (7,9,11,18). However, no method giving predictions in close agreement with measurements on beams has yet been presented, especially for the second and subsequent load cycles. The main reason seems to be the difficulty of accurately describing the behavior of concrete.

The aim of this study is to apply a new recently developed constitutive relation for concrete, called endochronic theory (4,5). This theory has been shown to

Note.—Discussion open until June 1, 1977. To extend the closing date one month, a written request must be filed with the Editor of Technical Publications, ASCE. This paper is part of the copyrighted Journal of the Structural Division, Proceedings of the American Society of Civil Engineers, Vol. 103, No. ST1, January, 1977. Manuscript was submitted for review for possible publication on May 4, 1976.

[1]Prof. of Civ. Engrg., Northwestern Univ., Evanston, Ill.

[2]Structural Engineer, Murphy Engineering Inc., Chicago, Ill.; formerly Grad. Student, Northwestern Univ., Evanston, Ill.

describe very well the response of plain concrete under cyclic loads and also under multiaxial stress; It can, therefore, be expected to be effective in the present problem.

The thick-beam bending theory with transverse shear will be adopted. Inclusion of shear can be important in large strain situations, even if the deflection due to shear is negligible, because inelastic shear strain produces volume dilatancy which, in turn, induces significant forces in the stirrups. Transverse normal strains will be introduced as separate variables, so as to allow consideration of the very important effects of the transverse normal stresses in concrete due to the confinement by stirrups. The effects of axial force in the beam will also be considered. Inclusion of transverse strains as variables represents an enhancement of the existing bending theories in which only curvature and transverse shear of beam are considered. For the purpose of numerical calculation, the cross section will be subdivided into layers, and each layer will be allowed to crack at different inclination, as determined from the normal stresses and the shear stresses in each layer. The crack closing, reopening, the formation of a secondary crack system, and the yielding, strain-hardening, and the Bauschinger effect in steel reinforcement, will be also modeled. A nonlinear stress-slip relation for bond deterioration should generally be included, but this is not done here as without it a satisfactory agreement with test data is obtained for the experiments considered. Apparently, anchorage of bars in these experiments was sufficient to prevent bond slip in the critical cross sections. However, analysis of other data may require consideration of bond deterioration, which is believed to have substantial effect in some cases.

Review of Endochronic Theory for Plain Concrete

The time independent form of the endochronic constitutive law for short time deformations of concrete (5) is

$$de_{ij} = \frac{ds_{ij}}{2G} + de''_{ij},\quad de''_{ij} = \frac{s_{ij}}{2G}\frac{d\zeta}{Z_1};\quad d\epsilon = \frac{d\sigma}{3K} + d\lambda \qquad (1)$$

in which $e_{ij} = \epsilon_{ij} - \delta_{ij}\epsilon$ = deviatoric components of strain tensor ϵ_{ij}; $\epsilon = (1/3)\epsilon_{kk}$ = volumetric strain; δ_{ij} = Kronecker delta; $s_{ij} = \sigma_{ij} - \delta_{ij}\sigma$ = deviatoric stress component of stress tensor σ_{ij}; $\sigma = (1/3)\sigma_{kk}$ = volumetric stress; subscripts i, j refer to Cartesian coordinates $x_i (i = 1, 2, 3)$; K, G = bulk and shear modulus; e''_{ij} = inelastic deviator strain; λ = inelastic dilatancy; Z_1 = constant; ζ = damage measure which is defined by

$$d\zeta = \frac{d\eta}{\left(1 + \dfrac{\beta_1\eta + \beta_2\eta^2}{1 + a_7 F_1}\right)F_2};\quad F_2 = 1 + \frac{a_8}{\left(1 + \dfrac{a_9}{\eta^2}\right)J_2(\underset{\sim}{\epsilon})} \qquad (2)$$

$$d\eta = \left\{\frac{a_0}{1 - [a_6 I_3(\underset{\sim}{\sigma})]^{1/3}} + F_1\right\} d\xi;\quad d\xi = \sqrt{\frac{1}{2}\, de_{ij}\, de_{ij}} \qquad (3)$$

$$F_1 = \frac{a_2[1 + a_5 I_2(\underset{\sim}{\sigma})]\sqrt{J_2(\underset{\sim}{\epsilon})}}{\{1 - a_1 I_1(\underset{\sim}{\sigma}) - [a_3 I_3(\underset{\sim}{\sigma})]^{1/3}\}[1 + a_4 I_2(\underset{\sim}{\sigma})\sqrt{J_2(\underset{\sim}{\epsilon})}]} \qquad (4)$$

Variable λ represents inelastic dilatancy, defined by

$$d\lambda = \frac{c_0}{1 - c_1 I_1(\underset{\sim}{\sigma})}\left(1 - \frac{\lambda}{\lambda_0}\right)\left\{\left(\frac{\lambda}{\lambda_0}\right)^2 + \left[\frac{J_2(\underset{\sim}{\epsilon})}{c_2^2 + J_2(\underset{\sim}{\epsilon})}\right]^3\right\} d\xi \qquad (5)$$

$$\text{and}\quad K = \frac{E_0}{3(1 - 2\nu)}\left(1 - \frac{\lambda}{4\lambda_0}\right);\quad G = \frac{E_0}{2(1 + \nu)}\left(1 - \frac{\lambda}{4\lambda_0}\right) \qquad (6)$$

in which I_1, I_2, and I_3 are the first, second, and third invariants of the tensor that follows in parentheses; and J_2 is the second invariant of the deviator. The following material parameters have been obtained by fitting numerous test data (5):

$$Z_1 = 0.0015;\quad \beta_1 = 30;\quad \beta_2 = 3500;\quad a_0 = 0.7;\quad a_1 = 0.6(f'_c)^{-1};$$

$$a_2 = 1400;\quad a_3 = 500(f'_c)^{-3};\quad a_4 = 475(f'_c)^{-2};\quad a_5 = 0.8(f'_c)^{-2};$$

$$a_6 = 0.055(f'_c)^{-3};\quad a_7 = 20;\quad a_8 = 0.000125;\quad a_9 = 0.0015;$$

$$\lambda_0 = 0.001;\quad c_0 = 1.0;\quad c_1 = 100(f'_c)^{-1};\quad c_2 = 0.0005;\quad \nu = 0.18;$$

$$E_0 = (0.565\ \text{psi} + 0.0001\, f'_c)\, 57{,}000\sqrt{f'_c}\ (\text{psi})^{-1/2}\ (1\ \text{psi} = 6.89\ \text{kN/m}^2) \qquad (7)$$

It is remarkable that, as a very good approximation, the preceding values apply for most normal-weight concretes (5). The value of the cylindrical compressive strength, f'_c, is the only parameter to be specified for the given concrete. The formulation in Eqs. 1-7 is fully continuous in that no inequalities are needed to distinguish between loading and unloading and various ranges of strain. For a simple explanation how the theory works for unloading, the reader may consult Fig. 1(*b*) of Ref. 5. The endochronic theory is particularly effective in modeling the cyclic response, the inelastic dilatancy due to large shear strains, the strain-softening properties, and hydrostatic pressure effect on triaxial behavior. It has been demonstrated (5) that the theory matches well the experimental uniaxial, biaxial, and triaxial stress-strain diagrams, including strain softening, and failure envelopes, torsion-compression tests, lateral stresses, volume change, unloading and reloading diagrams, and cyclic loading up to 10^6 cycles.

For numerical analysis it is more convenient to recast Eqs. 1 in a matrix form, which reads $\Delta\underset{\sim}{\sigma} + \Delta\underset{\sim}{\sigma}'' = \mathbf{D}\Delta\underset{\sim}{\epsilon}$, or

$$\begin{Bmatrix} \Delta\sigma_{11} + \Delta\sigma''_{11} \\ \Delta\sigma_{22} + \Delta\sigma''_{22} \\ \Delta\sigma_{33} + \Delta\sigma''_{33} \\ \Delta\sigma_{12} + \Delta\sigma''_{12} \\ \Delta\sigma_{23} + \Delta\sigma''_{23} \\ \Delta\sigma_{31} + \Delta\sigma''_{31} \end{Bmatrix} = \begin{bmatrix} D_{11} & D_{12} & D_{13} & 0 & 0 & 0 \\ & D_{22} & D_{23} & 0 & 0 & 0 \\ & & D_{33} & 0 & 0 & 0 \\ \text{symmetrical} & & & D_{44} & 0 & 0 \\ & & & & D_{55} & 0 \\ & & & & & D_{66} \end{bmatrix} \begin{Bmatrix} \Delta\epsilon_{11} \\ \Delta\epsilon_{22} \\ \Delta\epsilon_{33} \\ \Delta\epsilon_{12} \\ \Delta\epsilon_{23} \\ \Delta\epsilon_{31} \end{Bmatrix} \qquad (8)$$

in which $\Delta\sigma''_{ij} = 2G\Delta e''_{ij} + 3K\Delta\lambda\,\delta_{ij}$, δ_{ij} being Kronecker delta; and $D_{11} = D_{22} = D_{33} = K + 4G/3$, $D_{12} = D_{13} = D_{23} = K - 2G/3$, $D_{44} = D_{55} = D_{66} = 2G$.

These effects have been considered according to the present state-of-the-art (27,30). If the maximum principal stress, σ_{max}, exceeds a certain value (tensile strength f_t'), cracks are assumed to develop in the planes normal to the σ_{max} direction. To express this mathematically, an inelastic increment of σ_{max} equal $-f_t'$ must be introduced, so as to obtain zero normal stress on the crack planes, and the incremental stiffness matrix, **D**, must be replaced by a new matrix, **D'**. Before cracking, matrix **D** according to Eq. 8 is isotropic and, therefore, it applies for any coordinate axes, including those referred to principal stress directions. Assuming that there is only one crack system in which the cracks are open, matrix **D** is changed by cracking to the following incremental stiffness matrix:

$$\mathbf{D}' = \begin{bmatrix} 0 & 0 & 0 & 0 & 0 & 0 \\ & D_{22} - \frac{D_{12}^2}{D_{11}} & D_{23} - \frac{D_{13}D_{21}}{D_{11}} & 0 & 0 & 0 \\ & & D_{33} - \frac{D_{31}^2}{D_{11}} & 0 & 0 & 0 \\ & \text{symmetric} & & \alpha D_{44} & 0 & 0 \\ & & & & \alpha D_{55} & 0 \\ & & & & & D_{66} \end{bmatrix} \quad \ldots\ldots (9)$$

in which α = the shear transfer factor (27). Because matrix **D'** is orthotropic, it must be transformed from principal stress directions to the structural coordinate directions, x_i. This is accomplished as

$$\mathbf{D}'' = \mathbf{R}^T \mathbf{D}' \mathbf{R} \quad \ldots\ldots (10)$$

in which superscript T refers to a transpose and **R** = a (6 × 6) rotation matrix formed of the components of the fourth rank rotation tensor $[a_{kj}a_{li}]$, a_{ij} being the direction cosines of the principal stress directions:

$$\mathbf{R} = \begin{bmatrix} a_{11}^2 & a_{12}^2 & a_{13}^2 & a_{11}a_{12} & a_{12}a_{13} & a_{11}a_{13} \\ a_{21}^2 & a_{22}^2 & a_{23}^2 & a_{21}a_{22} & a_{22}a_{23} & a_{21}a_{23} \\ a_{31}^2 & a_{32}^2 & a_{33}^2 & a_{31}a_{32} & a_{32}a_{33} & a_{31}a_{33} \\ 2a_{11}a_{21} & 2a_{12}a_{22} & 2a_{13}a_{23} & a_{11}a_{22}+a_{12}a_{21} & a_{12}a_{23}+a_{13}a_{22} & a_{11}a_{23}+a_{13}a_{21} \\ 2a_{21}a_{31} & 2a_{22}a_{32} & 2a_{23}a_{33} & a_{21}a_{32}+a_{22}a_{31} & a_{22}a_{33}+a_{23}a_{32} & a_{21}a_{33}+a_{23}a_{31} \\ 2a_{11}a_{31} & 2a_{12}a_{32} & 2a_{13}a_{33} & a_{11}a_{32}+a_{12}a_{31} & a_{12}a_{33}+a_{13}a_{32} & a_{11}a_{33}+a_{13}a_{31} \end{bmatrix} \quad (11)$$

The shear transfer factor, α, describes the effect of aggregate interlock on rough surfaces of opened crack. Although this factor decreases with the opening of the crack and increases with the relative displacement parallel to the crack, an approximate constant value, $\alpha = 0.5$, seems to be sufficient for most practical purposes (27) and has been used in numerical calculations.

An open crack is assumed to close when the strain normal to the crack

becomes both less than the strain at which the crack has opened and less than zero (compression) (see Fig. 1). The formation of a secondary crack system

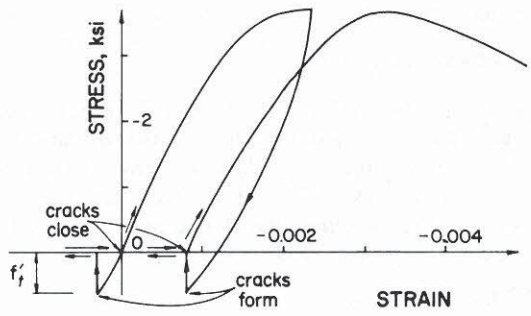

FIG. 1.—Stress-Strain Diagram for Concrete with Crack Opening and Crack Closing (1 ksi = 6.89 MN/m²)

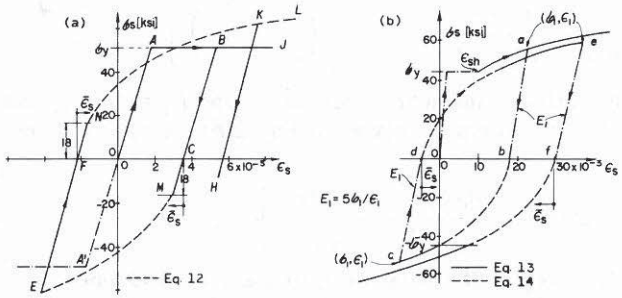

FIG. 2.—Stress-Strain Diagram for Reinforcing Steel (7,24) (1 ksi = 6.89 MN/m²)

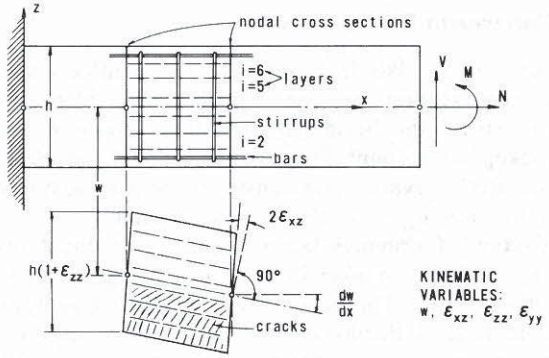

FIG. 3.—Deformation and Discretization of Beam

occurs again when the maximum principal stress exceeds tensile strength f_t'. If the first crack is still open, the secondary crack must be normal to the

first crack, unless aggregate interlock transmits appreciable shear stress; however, if the first crack has closed, then the secondary crack does not have to be normal to the first crack (9,11). If both cracks are open, then the incremental stiffness matrix is zero, $\mathbf{D}' = 0$.

Inelastic Behavior of Reinforcing Steel

For cyclic large strains, the reinforcing steel cannot be adequately represented by an elastic-plastic model (24) and the strain hardening and the Bauschinger effect must be taken into account (1,7). Various formulas have been developed for the strain-hardening curves (1,7,8). For steel that has not experienced strain-hardening on the first loading, the dotted segments in Fig. 2(*a*) in the subsequent strain cycles may be approximated by (1)

$$|\sigma_s| = 64.5 - 52.7(0.838)^{1{,}000\bar{\epsilon}_s} \text{ ksi} \quad \ldots\ldots\ldots\ldots\ldots\ldots\ldots\ldots \quad (12)$$

in which 1 ksi = 6.895 MN/m^2; and $\bar{\epsilon}_s$ is defined in Fig. 2(*a*). For steel that experiences strain-hardening in the first cycle, the solid line segment in Fig. 2(*b*) is approximated (in ksi) by (7,8)

$$\sigma_s = \sigma_y \left[\frac{112(\epsilon_s - \epsilon_{sh}) + 2}{60(\epsilon_s - \epsilon_{sh}) + 2} + \frac{\epsilon_s - \epsilon_{sh}}{\epsilon_u - \epsilon_{sh}} \left(\frac{\sigma_u}{\sigma_y} - 1.7 \right) \right] \quad \ldots\ldots\ldots\ldots \quad (13)$$

The straight (dash-dot) unloading lines have slope $E_1 \approx 5\sigma_1/\epsilon_1$ and the dashed line segments for subsequent cycles in Fig. 2(*b*) are approximated (in ksi) by (7)

$$\sigma_s = \sigma_y \left[1 - \exp\left(-\frac{2.05\,\bar{\epsilon}_s}{\epsilon'_{sh}} \right) + \frac{0.129\,\bar{\epsilon}_s}{\epsilon'_{sh}} \right] \quad \ldots\ldots\ldots\ldots\ldots \quad (14)$$

in which $\epsilon'_{sh} = (\epsilon_{sh}/1.38) \ln (\epsilon_{ip}/\epsilon_y)$; (σ_y, ϵ_y) = yield point; ϵ_u = strain at ultimate stress at first loading; $\bar{\epsilon}_s$, ϵ_{sh} is defined in Fig. 2(*b*); (σ_1, ϵ_1) = reversal points in Fig. 2(*b*); and ϵ_{ip} = strain between successive points of zero stress immediately preceding a given cycle.

Internal Force-Displacement Relations for Beam

Consider a beam whose axis is x and cross-sectional coordinates are y and z (Fig. 3). The cross sections are assumed to remain plane, but not normal to the deflected axis of the beam, so that shear strains ϵ_{xz} and ϵ_{xy} due to bending may be taken into account. They are considered to be constant throughout each cross section. Both curvature and transverse shear are assumed to contribute to deflections. (Notation: $\epsilon_{xz} = \gamma_{xz}/2$, γ_{xz} = shear angle.)

As a generalization of previous beam formulations, the transverse normal strains, ϵ_{yy} and ϵ_{zz}, will be also taken into account, being assumed to be constant throughout the cross section. This is very important for the analysis of reinforced concrete beams at large deflections, because the large lateral strains due to high longitudinal compression are opposed by stirrups, and the force in the stirrups introduces into concrete a lateral confining stress, which considerably strengthens concrete for longitudinal compression. Consideration of ϵ_{yy} and ϵ_{zz} would have been, of course, meaningless without a stress-strain law that realistically describes lateral strains and volume changes due to deviator strains and the hydrostatic pressure sensitivity.

The bending is supposed to occur in the direction of axis z. The cross section of the beam is subdivided in the z direction into layers $i = 1, 2, \ldots n$ of cross-sectional areas A_i and centroidal coordinates z_i (Fig. 3). The levels of longitudinal steel reinforcement layers are denoted as z_{s_j}, $j = 1, 2, \ldots$. Although bond slip is undoubtedly of importance in cases of weak anchorage of reinforcement, here perfect bond is assumed to exist, and so the strains in steel and concrete are equal. The longitudinal normal strain increment at any point of the cross section is

$$d\epsilon_{xx} = d\epsilon_0 - z\,dk \quad \ldots\ldots\ldots\ldots\ldots\ldots\ldots\ldots\ldots\ldots\ldots\ldots \quad (15)$$

in which ϵ_0 = normal strain ϵ_{xx} at the chosen beam axis, x; k = curvature of beam; and $\epsilon_{xx} = \epsilon_{11}$, subscripts x, y, z being used interchangeably with 1, 2, 3. Substituting Eq. 15 into the stress-strain relation in the form of Eq. 8, and setting $\epsilon_{xy} = \epsilon_{yz} = \sigma_{xy} = \sigma_{yz} = 0$, one obtains expressions for $d\sigma_{xx}$, $d\sigma_{yy}$, $d\sigma_{zz}$, and $d\sigma_{xz}$ in terms of $d\epsilon_0$, dk, $d\epsilon_{yy}$, $d\epsilon_{zz}$, and $d\epsilon_{xz}$. If these expressions are further substituted into the approximate equilibrium relations:

$$\Delta M^c = \sum_i z_i A_i \Delta\sigma_{xx_i}; \quad \Delta N^c_x = \sum_i A_i \Delta\sigma_{xx_i}; \quad \Delta N^c_y = \sum_i A_{y_i} \Delta\sigma_{yy_i};$$

$$\Delta N^c_z = \sum_i A_{z_i} \Delta\sigma_{zz_i}; \quad \Delta V^c = \sum_i A_i \Delta\sigma_{xz_i} \quad \ldots\ldots\ldots\ldots\ldots\ldots\ldots \quad (16)$$

it follows that

$$\Delta\mathbf{f}^c = \mathbf{R}^c \Delta\mathbf{d} - \Delta\mathbf{f}'' \quad \ldots\ldots\ldots\ldots\ldots\ldots\ldots\ldots\ldots\ldots\ldots\ldots \quad (17)$$

Here, M^c = bending moment in concrete about axis y (Fig. 3); N^c_x, N^c_y, N^c_z = normal forces in concrete in x, y, and z directions; V^c = shear force in concrete in direction z; subscript i refers to layers $i = 1, 2, \ldots n$; A_{y_i}, A_{z_i} = areas of concrete in layer i per unit length of beam in planes xz and xy; and

$$\mathbf{f}^c = \begin{Bmatrix} M^c \\ N^c_x \\ N^c_y \\ N^c_z \\ V^c \end{Bmatrix}; \quad \mathbf{d} = \begin{Bmatrix} k \\ \epsilon_0 \\ \epsilon_{yy} \\ \epsilon_{zz} \\ \epsilon_{xz} \end{Bmatrix}; \quad \Delta\mathbf{f}'' = \sum_i \begin{Bmatrix} A_i z_i \Delta\sigma''_{xx_i} \\ A_i \Delta\sigma''_{xx_i} \\ A_{y_i} \Delta\sigma''_{yy_i} \\ A_{z_i} \Delta\sigma''_{zz_i} \\ A_i \Delta\sigma''_{xz_i} \end{Bmatrix} \quad \ldots\ldots\ldots \quad (18)$$

$$\mathbf{R}^c = \sum_i \begin{bmatrix} -A_i z_i^2 D''_{11} & A_i z_i D''_{11} & A_i z_i D''_{12} & A_i z_i D''_{13} & 0 \\ -A_i z_i D''_{11} & A_i D''_{11} & A_i D''_{12} & A_i D''_{13} & 0 \\ -A_{y_i} z_i D''_{21} & A_{y_i} D''_{21} & A_{y_i} D''_{22} & A_{y_i} D''_{23} & 0 \\ -A_{z_i} z_i D''_{31} & A_{z_i} D''_{31} & A_{z_i} D''_{32} & A_{z_i} D''_{33} & 0 \\ 0 & 0 & 0 & 0 & A_i D''_{66} \end{bmatrix} \quad \ldots\ldots \quad (19)$$

in which D''_{kl} is given by Eq. 10 (with account of cracking) and $D''_{kl} = D_{kl}$ in case that no crack exists, $\mathbf{R}_c$ = stiffness matrix due to concrete alone. The force increments due to layers ($j = 1, 2, \ldots$) of reinforcement are $\Delta\mathbf{f}^s = \mathbf{R}^s\Delta\mathbf{d}$, in which $\mathbf{f}^s$ = matrix analogous to $\mathbf{f}^c$ and

$$\mathbf{R}^s = \sum_j \begin{bmatrix} -A_{s_j}E_{s_j}z_{s_j}^2 & A_{s_j}E_{s_j}z_{s_j} & 0 & 0 & 0 \\ -A_{s_j}E_{s_j}z_{s_j} & A_{s_j}E_{s_j} & 0 & 0 & 0 \\ 0 & 0 & \frac{2}{a}A_{st}E_{st} & 0 & 0 \\ 0 & 0 & 0 & \frac{2}{a}A_{st}E_{st} & 0 \\ 0 & 0 & 0 & 0 & 0 \end{bmatrix} \quad \ldots\ (20)$$

in which subscript *st* refers to stirrups while *s* refers to longitudinal reinforcement; a = stirrup spacing; $2A_{st}$ = cross-sectional area of stirrups; and E_s, E_{st} = tangent modulus of longitudinal steel and of stirrups, which is calculated using Eqs. 12–14.

The total forces in the cross section are obtained by summing the contributions of concrete and steel, Eqs. 17 and 20. This yields

$$\Delta\mathbf{f} = \mathbf{R}\,\Delta\mathbf{d} - \Delta\mathbf{f}''; \quad \mathbf{R} = \mathbf{R}^c + \mathbf{R}^s \quad \ldots\ (21)$$

in which $\mathbf{f}$ = matrix analogous to $\mathbf{f}^c$, Eq. 18, but without superscript *c*. Eq. 21 represents the force-displacement relations for a cross section of the beam.

For convergence of the iterative step-by-step computation of beam response, specification of displacement increments, rather than force increments, is desirable, as far as possible. For this reason, it is convenient to switch between the left and right-hand sides the terms with Δk and ΔM in the five equations that result when the matrix equation, Eq. 21, is rewritten in the component form. This provides

$$\begin{bmatrix} -1 & R_{12} & R_{13} & R_{14} & R_{15} \\ 0 & R_{22} & R_{23} & R_{24} & R_{25} \\ 0 & R_{32} & R_{33} & R_{34} & R_{35} \\ 0 & R_{42} & R_{43} & R_{44} & R_{45} \\ 0 & R_{52} & R_{53} & R_{54} & R_{55} \end{bmatrix} \begin{Bmatrix} \Delta M \\ \Delta\epsilon_0 \\ \Delta\epsilon_{yy} \\ \Delta\epsilon_{zz} \\ \Delta\epsilon_{xz} \end{Bmatrix} = \begin{bmatrix} -R_{11}\Delta k - \Delta f''_1 \\ \Delta N_x - R_{21}\Delta k - \Delta f''_2 \\ \Delta N_y - R_{31}\Delta k - \Delta f''_3 \\ \Delta N_z - R_{41}\Delta k - \Delta f''_4 \\ \Delta V - R_{51}\Delta k - \Delta f''_5 \end{bmatrix} \quad \ldots\ (22)$$

in which R_{kl} = components of matrix $\mathbf{R}$ from Eq. 21.

Computation of Moment-Curvature Relations

Test data on cyclic behavior of reinforced concrete beams have been reported in terms of moment-curvature relations, moment-rotation relations, or load-deflection relations. Because of the coupling between shear strain and inelastic dilatancy, shear force V needs to be considered also. The controlled variable in the tests is the load on the beam, which determines both M and V, and the measured variable is the deflection, which specifies curvature k. However,

as long as creep is not considered, it is also possible to consider that the specified increments are Δk and ΔV, rather than ΔM and ΔV, and that ΔM is the response, as is indicated in Eq. 22. This gives faster convergence of the iterations in each loading step. Further variables that are specified by the loading method are ΔN_x, ΔN_y, and ΔN_z; usually $\Delta N_y = \Delta N_z = 0$, i.e., the complete right-hand side column vector in Eq. 22 is given at each loading step.

To achieve better convergence, curvature increments were used as the input and bending moments were calculated as the response, as explained before Eq. 22. This cannot be, however, implemented to the full extent in cases where the deflection was measured instead of the curvature. Yet, in such cases, it was possible (and rather beneficial for convergence) to specify as input the curvature increments at least at the maximum moment cross section (the beam being statically determinate). By iterative solution of Eq. 21 and the equilibrium relation between maximum moment and corresponding shear force, the curvature, shear force, and shear angle at that cross section was found at each step. The bending moment and shear force at every other cross section could then be determined merely from equilibrium relations. These were then used as input values for the calculation of curvature and shear angle from Eq. 21 at every other section. Then, using curvatures and shear angles at all cross sections, the deflection was calculated by numerical integration and was compared at each loading step with the recorded deflections in tests; loading was reversed to unloading whenever the extreme reported deflection for the cycle was reached or exceeded.

For vectors $\mathbf{f}$ and $\mathbf{d}$, both the values at the beginning of the step (subscript r) and the increments during the step (r, $r + 1$) from the previous iteration must be stored. In addition, the same must be stored for all values σ_{xx_i} and σ_{xz_i} and for the stresses in longitudinal steel and the stirrups. (The normal strains and their increments in any layer are always evaluated from $\epsilon_{xx} = \epsilon_0 - zk$.) The computational algorithm in each loading step (r, $r + 1$) may proceed as follows:

1. For all layers, assume that $\Delta\mathbf{f}$, $\Delta\mathbf{d}$, $\Delta\sigma_{xx_i}$, and $\Delta\sigma_{xz_i}$ are the same as in the previous iteration, or, in case of first iteration, same as in the previous step.
2. Evaluate $\mathbf{f}_{r+(1/2)} = \mathbf{f}_r + (1/2)\Delta\mathbf{f}$, etc., for the midstep and, using central difference approximations, evaluate $\Delta\xi$, $\Delta\eta$, $\eta_{r+(1/2)}$, $\Delta\zeta$, $\Delta e''_{ij}$, $\Delta\lambda$, $\Delta\sigma''_{ij}$, $\mathbf{D} = [D_{kl}]_{r+(1/2)}$ for all layers.
3. Taking into account the cracks (if any), possibly existing at the beginning of the step, evaluate $\mathbf{D}'_{r+(1/2)}$ (Eq. 9) and $\mathbf{D}''_{r+(1/2)}$ (Eq. 10).
4. Evaluating strains in steel with the help of k and ϵ_0, and noting the number of cycles, calculate the tangent moduli for longitudinal steel layer and horizontal and vertical stirrups (Eqs. 12–14).
5. Calculate $\Delta\mathbf{f}''$ (Eq. 18), $\mathbf{R}^c_{r+(1/2)}$ (Eq. 19), $\mathbf{R}^s_{r+(1/2)}$ (Eq. 20), $\mathbf{R}_{r+(1/2)}$ (Eq. 21), and the matrix of Eq. 22.
6. Solve ΔM, $\Delta\epsilon_0$, $\Delta\epsilon_{yy}$, $\Delta\epsilon_{zz}$, $\Delta\epsilon_{xz}$ from Eq. 22.
7. Evaluate the final stresses, $\sigma_{xx_{r+1}} = \sigma_{xx_r} + \Delta\sigma_{xx}$, etc., and the principal stresses for all layers at the end of step. Check the conditions of cracking and crack closing for each layer and record whether cracks are open or closed. If cracks have not existed at the beginning of the step and have formed during

the step, record the inclinations, α_i, of the cracks.

8. Compare the values ΔM, $\Delta\epsilon_0$, $\Delta\epsilon_{yy}$, $\Delta\epsilon_{zz}$, $\Delta\epsilon_{xz}$ with those from the previous iteration. If any of the differences is more than a specified percentage, return to stage 1 and iterate the whole procedure; otherwise proceed to the next step ($r + 1$, $r + 2$). Note that when more than four iterations would be required,

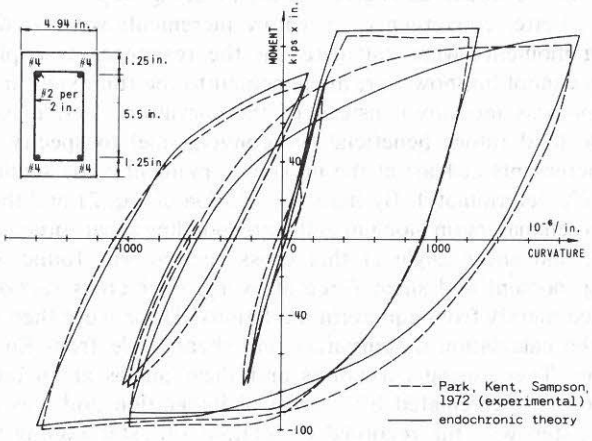

FIG. 4.—Fit of Moment-Curvature Test for Concrete Beam (18) (1 kip = 4.45 kN; 1 in. = 25.4 mm)

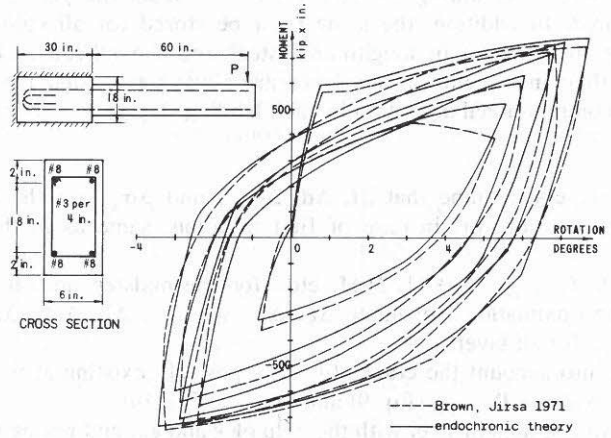

FIG. 5.—Fit of Moment-Rotation Test for Concrete Beam (7) (1 kip = 4.45 kN; 1 in. = 25.4 mm)

it is more efficient to decrease the load increment.

If cracks form during the current step, the increments of principal stress, σ_I^a, across the crack plane will be zero in subsequent steps. However, in the current step the increment of σ_I^a does not lead to exactly zero value of σ_I^a at $r + 1$, unless cracks form exactly at stage $r + 1$ and not between stages

r and $r + 1$. Neglection of this fact represents a numerical error. (The error could be removed if various sizes of the current step were tried until the final value of σ_I^a was made as small as desired.)

Numerical Predictions and Comparison with Tests

Test results are available in the form of moment-curvature, moment-rotation or load-deflection curves. In case of the tests by Park, et al. (18) the moment and curvature have been reported for the midsection of a simply supported beam. The results of the numerical predictions are shown by solid lines in Fig. 4. In case of the tests by Brown and Jirsa (7), Fig. 5, moment-rotation curves are given for a cantilever beam fixed at one end. Noting that cross sections that are more than distance d away from the fixed end remain elastic,

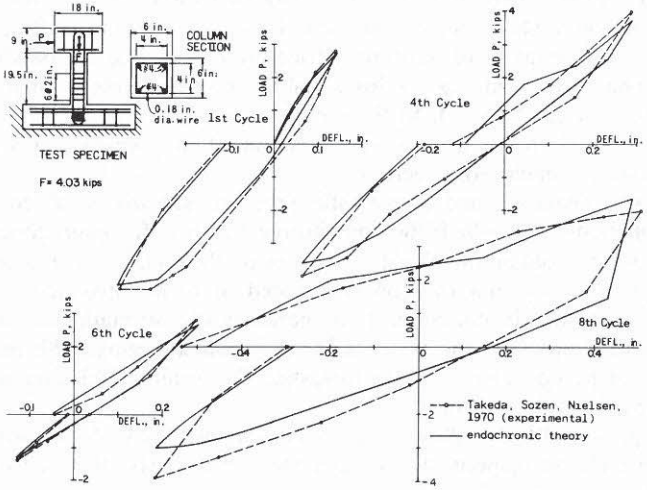

FIG. 6.—Fit of Load-Deflection Test for Concrete Beam (28) (1 kip = 4.45 kN; 1 in. = 25.4 mm)

the rotation at the other end has been obtained by calculating the curvature for the cross sections at distances 0, $d/2$, and d from the fixed end, where d is the effective depth of the beam, and then using the trapezoidal rule to integrate between 0 and d and considering a linear variation of curvature over the rest of the beam. Transverse shears have been also included (Fig. 3); they have no effect on end rotation but influence indirectly the curvatures by means of the constitutive law. Similar numerical integration has been performed for the tests by Takeda, Sozen, and Nielsen (28), Fig. 6, and the deflection has been obtained by integrating curvatures and shear angles. Cross sections have been subdivided in nine layers of equal depth (Fig. 3). The cross section area of longitudinal bars was subtracted from the area of concrete. However, the cross section area of stirrups has not been subtracted.

The agreement of the theoretical predictions with the test data in Figs. 4–6 is seen to be very close.

Conclusions

1. The most remarkable result is the fact that the endochronic theory has correctly predicted the response of reinforced concrete members under cyclic loading, without needing to adjust any values of the material parameters determined previously from tests of plain concrete (5). Thus, the endochronic theory represents not merely a descriptive model, but a prediction method. This is of great value for extrapolations from available test data and reduces the need for obtaining experimental data for each particular structure.

2. When the theory of bending, based on the assumption of planar cross sections, is applied to inelastic behavior, the transverse shear strains must be included even if the shear deflection is negligible because the inelastic shear strains (associated with microcracking) give rise to volumetric dilatancy which induces significant forces in the stirrups, as well as longitudinal bars.

3. In the existing theories of bending, only two variables, i.e., the curvature and the transverse shear angle, are used. However, this is insufficient in the case of inelastic behavior of reinforced concrete beams, and the bending theory must be enhanced by adding a third variable, the transverse normal strain (or the transverse normal stress). In three-dimensional analysis, this means adding transverse normal strains in two transverse directions, which yields a total of four variables for each cross section.

4. Inelastic dilatancy and hydrostatic pressure sensitivity of concrete are essential phenomenons which the constitutive equation for plain concrete must exhibit in order to obtain the effect of stirrups on the inelastic response. Stirrups oppose the dilatancy and the forces induced in them introduce a confining hydrostatic pressure in concrete. This increases the strength and ductility of concrete and suppresses the appearance of strain-softening. The response of stirrups must be considered as elastoplastic. The same conclusion would also apply to spiral reinforcement.

5. The present theory allows the cross-sectional area of stirrups required for ductile inelastic response to be calculated. Previously, this had to be done empirically.

6. The present method is applicable to arbitrary histories of bending moment, axial force, and shear force.

7. As far as the role of concrete under compression is concerned, the mathematical model is fully continuous in that, by contrast with previous models, no inequalities are needed to distinguish between loading and unloading and various ranges of strain. The continuity property makes extrapolations more reliable.

Acknowledgment

The development of the endochronic theory and its application to beams has been funded by Grants GK-26030 and ENG75-14848 from the National Science Foundation and a Northwestern University subcontract for Energy Research and Development Administration under contract with Union Carbide Corp. through Oak Ridge National Laboratory.

Appendix I.—Further Information on Experimental Data

Fig. 4.—Concrete: f'_c = 6,950 psi (47.9 N/mm^2), f'_t assumed as = 500 psi (3.45 N/mm^2); Top steel: σ_y = 47,500 psi (327 N/mm^2), σ_u = 68,500 psi (472 N/mm^2), ϵ_{sh} = 0.0336 for bottom steel; σ_y = 49,200 psi (339 N/mm^2), σ_u = 69,700 psi (481 N/mm^2), ϵ_{sh} = 0.0323. The beam is simply supported at ends; moment and curvature is measured at midsection.

Fig. 5.—Concrete: f'_c = 4,800 psi to 6,200 psi [f'_c = 5,000 psi (34.42 N/mm^2) and f'_t = 450 psi (3.1 N/mm^2) is used for the fit]. Steel: σ_y = 46 ksi (316.66 N/mm^2), ϵ_{sh} = 0.008 to 0.014 (taken as 0.01 for the fit), σ_u = 79 ksi (543.84 N/mm^2), ϵ_u = 0.2.

Fig. 6.—Concrete: f'_c = 4,830 psi (33.25 N/mm^2); f'_t = 420 psi (2.89 N/mm^2) Steel: σ_y = 51,000 psi (351 N/mm^2), ϵ_{sh} = 0.015, σ_{yst} = 40,000 psi (275.36 N/mm^2); axial load = 4,030 lb (17,925 N).

Appendix II.—References

1. Agrawal, G. L., Tulin, L. G., and Gerstle, K. H., "Response of Doubly Reinforced Concrete Beams to Cyclic Loading," *American Concrete Institute Journal*, Vol. 62, No. 7, July, 1965, pp. 823-836.
2. Aktan, A. E., and Pecknold, D. A. W., "Response of a Reinforced Concrete Section to Two-Dimensional Curvature Histories," *American Concrete Institute Journal*, Vol. 71, No. 5, May, 1974, pp. 246-250.
3. Aoyama, H., "Moment-Curvature Characteristics of Reinforced Concrete Members Subjected to Axial Load and Reversal of Bending," *Proceedings*, International Symposium on the Flexural Mechanics of Reinforced Concrete, held at Miami, Fla., Nov., 1964, *American Concrete Institute Special Publication No. 12*, Detroit, Mich., 1965, pp. 183-212.
4. Bažant, Z. P., "A New Approach to Inelasticity and Failure of Concrete, Sand, and Rock: Endochronic Theory" (Abstract), *Proceedings*, Society of Engineering Science, 11th Annual Meeting, G. J. Dvorak, ed., Duke University, Durham, N. C., Nov., 1974, pp. 158-159.
5. Bažant, Z. P., and Bhat, P. D., "Endochronic Theory of Inelasticity and Failure of Concrete," *Journal of the Engineering Mechanics Division*, ASCE, Vol. 102, No. EM4, Proc. Paper 12360, Aug., 1976, pp. 701-722.
6. Bertero, V. V., and Bresler, B., "Seismic Behavior of Reinforced Concrete Framed Structures," *Proceedings*, Fourth World Conference on Earthquake Engineering, Santiago, Chile, Vol. 1, B-2, 1969, pp. 109-124.
7. Brown, R. H., and Jirsa, J. O., "Reinforced Concrete Beams under Load Reversals," *American Concrete Institute Journal*, Vol. 68, May, 1971, pp. 380-390.
8. Burns, N. H., and Siess, C. P., "Repeated and Reversed Loading in Reinforced Concrete," *Journal of the Structural Division*, ASCE, Vol. 92, No. ST5, Proc. Paper 4932, Oct., 1966, pp. 65-78.
9. Červenka, V., and Gerstle, K. H., "Inelastic Analysis of Reinforced Concrete Panels," *Publications*, International Association for Bridge and Structural Engineering, Zürich, Switzerland, Vol. 31, 1971, pp. 31-45, and Vol. 32, 1972, pp. 25-39.
10. Clough, R., and Johnston, S., "Effect of Stiffness Degradation on Earthquake Ductility Requirements," *Proceedings of Japan Earthquake Engineering Symposium*, Tokyo, Japan, 1966, pp. 227-232.
11. Darwin, D., and Pecknold, D. A., "Analysis of RC Shear Panels Under Cyclic Loading," *Journal of the Structural Division*, ASCE, Vol. 102, No. ST2, Proc. Paper 11896, Feb., 1976, pp. 355-369.
12. Gerstle, K. H., and Tulin, L. G., "Incremental Deformations of Under-Reinforced Concrete Beams," *Magazine of Concrete Research*, Vol. 23, No. 77, Dec., 1971, pp. 161-168.
13. Hand, F. R., Pecknold, D. A., and Schnobrich, W. C., "Nonlinear Layered Analysis of RC Plates and Shells," *Journal of the Structural Division*, ASCE, Vol. 99, No. ST7, Proc. Paper 9860, July, 1973, pp. 1491-1505.
14. Jofriet, J. C., and McNeice, G. M., "Finite Element Analysis of Reinforced Concrete

Slabs," *Journal of the Structural Division*, ASCE, Vol. 97, No. ST3, Proc. Paper 7963, Mar., 1971, pp. 785-806.
15. Lin, C. S., and Scordelis, A. C., "Nonlinear Analysis of RC Shells of General Form," *Journal of the Structural Division*, ASCE, Vol. 101, No. ST3, Proc. Paper 11164, Mar., 1975, pp. 523-538.
16. Ngo, D., and Scordelis, A. C., "Finite Element Analysis of Reinforced Concrete Beams," *American Concrete Institute Journal*, Vol. 64, No. 3, Mar., 1967, pp. 152-163.
17. Nilson, A. H., "Nonlinear Analysis of Reinforced Concrete by Finite Elements," *American Concrete Institute Journal*, Vol. 65, Sept., 1968, pp. 757-766.
18. Park, R., Kent, D. C., and Sampson, R. A., "Reinforced Concrete Members with Cyclic Loading," *Journal of the Structural Division*, ASCE, Vol. 98, No. ST7, Proc. Paper 9011, July, 1972, pp. 1341-1360.
19. Rashid, Y. R., "Analysis of Prestressed Concrete Pressure Vessels," *Nuclear Engineering and Design*, Vol. 7, No. 4, Apr., 1968, pp. 334-344.
20. Ruiz, W. M., and Winter, G., "Reinforced Concrete Beams under Repeated Loads," *Journal of the Structural Division*, ASCE, Vol. 95, No. ST6, Proc. Paper 6601, June, 1969, pp. 1189-1211.
21. Rumman, W. S., and Sun, R. T., "Hysteresis Loops of Reinforced Concrete Elements Subjected to Reversed Cyclic Axial Loading," *Final Report*, Symposium on Resistance and Ultimate Deformability of Structures Acted on by Well Defined Repeated Loads, International Association of Bridge and Structural Engineering, Vol. 14, (held in Lisbon, Portugal), Zürich, Switzerland, 1973, pp. 59-64.
22. Schnobrich, W. C., et al., Discussion of "Nonlinear Stress Analysis of Reinforced Concrete," by S. Valliappan and T. F. Doolan, *Journal of the Structural Division*, ASCE, Vol. 98, No. ST10, Proc. Paper 9227, Oct., 1972, pp. 2327-2328.
23. Scordelis, A. C., "Finite Element Analysis of Reinforced Concrete Structures," Specialty Conference on the Finite Element Methods in Civil Engineering, McGill University, Montreal, Quebec, Canada, 1972, pp. 71-113.
24. Singh, A., Gerstle, K. H., and Tulin, L. G., "The Behavior of Reinforcing Steel under Reversed Loading," *Materials Research and Standards*, American Society for Testing and Materials, Vol. 5, No. 1, Jan., 1965, pp. 12-17.
25. Singh, H. N., Gerstle, K. H., and Tulin, L. G., "Shear Strength of Concrete Beams under Cyclic Loading—A Preliminary Study," *Symposium on Resistance and Ultimate Deformability of Structures Acted on by Well Defined Repeated Loads*, International Association of Bridge and Structural Engineering, Vol. 13, (held in Lisbon, Portugal), Zürich, Switzerland, 1973, pp. 61-65.
26. Sinha, B. P., Gerstle, K. H., and Tulin, L. G., "Response of Singly Reinforced Beams to Cyclic Loading," *American Concrete Institute Journal*, Vol. 61, No. 8, Aug., 1964, pp. 1021-1037.
27. Suidan, M., and Schnobrich, W. C., "Finite Element Analysis of Reinforced Concrete," *Journal of the Structural Division*, ASCE, Vol. 99, No. ST10, Proc. Paper 10081, Oct., 1973, pp. 2109-2122.
28. Takeda, T., Sozen, M. A., and Nielsen, N. N., "Reinforced Concrete Response to Simulated Earthquakes," *Journal of the Structural Division*, ASCE, Vol. 96, No. ST12, Proc. Paper 7759, Dec., 1970, pp. 2557-2573.
29. Valliappan, S., and Doolan, T. F., "Nonlinear Stress Analysis of Reinforced Concrete," *Journal of the Structural Division*, ASCE, Vol. 98, No. ST4, Proc. Paper 8845, Apr., 1972, pp. 885-898.
30. Yuzugullu, O., and Schnobrich, W. C., "A Numerical Procedure for the Determination of the Behavior of a Shear Wall Frame System," *American Concrete Institute Journal*, Vol. 70, No. 7, July, 1973, pp. 474-479.

Appendix III.—Notation

The following symbols are used in this paper:

A, A_y, A_z = cross-sectional area of concrete element along x, y, and z directions;

A_{st} = cross-sectional area of stirrups;
a = spacing of shear stirrups in beam;
$a_0, \ldots a_9$ = material constants in Eq. 7;
c_0, c_1, c_2 = material constants in Eq. 5;
E_s = tangent modulus of reinforcing steel;
E_{st} = tangent modulus of stirrups;
e_{ij}, de''_{ij} = deviator of strain tensor ϵ_{ij} and its inelastic increments;
f'_c, f'_t = strength of concrete in compression and tension;
G, K = elastic shear modulus and bulk modulus;
I_1, I_2, I_3 = first, second, and third invariants of tensor that follows in parentheses;
J_2 = second invariant of deviator of tensor that follows in parentheses;
k = curvature of beam;
M = bending moment at section of beam (Fig. 3);
N_x, N_y, N_z = normal forces at section along x, y, and z directions;
P = load on beam causing bending moment;
s_{ij} = deviator of stress tensor σ_{ij};
V = shear force at section of beam;
Z_1 = constant = relaxation strain (Eq. 1);
z_i = distance to centroid of ith layer from axis of beam (Fig. 3);
z_{sj} = distance to longitudinal steel layer j, from axis of beam;
α = shear transfer factor (Eq. 9);
β_1, β_2 = constants = strain hardening parameters (Eq. 7);
δ_{ij} = Kronecker delta;
ϵ_0 = normal strain along axis of beam;
$\epsilon_{ij}, \underset{\sim}{\epsilon}$ = strain tensor (linearized);
$\epsilon_s, \epsilon_{sh}, \epsilon_u, \epsilon_y$ = strain, strain-hardening, ultimate strain and yield strain in reinforcing steel;
$\bar{\epsilon}_s, \epsilon'_{sh}, \epsilon_{ip}$ = various strains in steel defined by Eqs. 12-14 and Figs. 2(a) and 2(b);
ζ = damage measure (Eq. 2);
η = internal deformation measure in Eqs. 2 and 3;
λ, λ_0 = inelastic dilatancy and its maximum possible value (Eq. 5);
ξ = distorsion measure (Eq. 3);
ρ = reinforcement ratio;
$\sigma_{ij}, \underset{\sim}{\sigma}$ = stress tensor; and
$\sigma_s, \sigma_u, \sigma_y$ = stress, ultimate stress, and yield stress in steel.

Subscripts

i = layer of concrete in beam cross section;
j = longitudinal steel locations in beam;
r = loading step ending at time t_r; and
$r - (1/2)$ = average in step (t_{r-1}, t_r).

Superscripts

c = concrete; and
s = steel.

12662 HYSTERESIS OF R.C. MEMBERS

KEY WORDS: **Bauschinger effect; Beams (supports); Columns (supports); Concrete (reinforced);** Cyclic loads; Damping; Ductility; Earthquake loads; Earthquakes; Failure; **Hysteresis; Inelastic action;** Nonlinear systems; Plasticity; Stirrups

ABSTRACT: The endochronic theory for inelasticity and failure, previously established, is used to predict the response of reinforced concrete beams in cyclic bending at large strains. Cross sections are assumed to remain plain and are subdivided in slices. Existing bending theories must be enhanced by inclusion of transverse normal strain as a third variable, in addition to curvature and transverse shear angle. The forces in stirrups bring concrete under confining hydrostatic pressure, and, according to endochronic theory, this greatly increases ductility and strength and suppresses strain-softening. The theory is applicable to any history of bending moment, shear force, and axial force, and allows the necessary cross-sectional area of stirrups to be calculated. It is most remarkable that a number of test data have been correctly predicted without having to adjust any of the material parameters determined previously from tests of plain concrete. The endochronic theory represents not merely a descriptive model, but a prediction method.

REFERENCE: Bazant, Zdenek P., and Bhat, Parameshwara D., "Prediction of Hysteresis of Reinforced Concrete Members," *Journal of the Structural Division,* ASCE, Vol. 103, No. ST1, **Proc. Paper 12662**, January, 1977, pp. 153-167